

# The Architecture of Perceptual Spatial Interactions

URI POLAT,\* DOV SAGI\*

Received 24 December 1992; in revised form 6 April 1993

---

**Lateral interactions between spatial filters were explored with a lateral masking paradigm. Contrast sensitivity (two-alternative forced-choice) for a Gabor signal in the presence of two flanking high contrast Gabor signals (masks) was measured. When the target to mask distance was less than 2 target wavelengths the contrast sensitivity decreased up to a factor of two relative to a no mask condition. At larger separations, up to eight wavelengths, an increase in contrast sensitivity occurred. This increase was maximal at separation distances of 2–3 wavelengths, where sensitivity increased by a factor of two. However, the enhancement magnitude and range was dependent on the offset between the Gabor signal orientation and the direction defined by the virtual line connecting the two masks (global orientation). Maximal effects occurred when this offset was zero (100% increase in sensitivity) and 90 deg (50% increase). A 45 deg offset yielded only a small enhancement (20%). The enhancement dependence on spatial arrangement was found to be invariant across different global orientations (meridian). This pattern of interactions may be involved in grouping collinear line segments into smooth curves.**

Lateral masking Gabor Contrast sensitivity Global orientation

---

## 1. INTRODUCTION

Due to the local nature of spatial filters, some visual processes may involve interactions between neighboring channels. Studies involving subjective contrast estimations yield experimental evidence for local spatial interactions (Cannon & Fullenkamp, 1991; Chubb, Sperling & Solomon, 1989; Sagi & Hochstein, 1985). Thus, the existence of local inhibitory connections between spatial filters having similar orientation and spatial frequency selectivity was suggested (Sagi, 1990). An antagonistic connectivity field around each channel having excitatory and inhibitory connections, is observed when measuring contrast detection thresholds for a foveal Gabor signal flanked by two high contrast Gabor signals (Polat & Sagi, 1993). The results showed a suppressive region extending to a radius of 2 wavelengths, in which the presence of the masking signals has the effect of increasing the target threshold, beyond this range a much larger facilitatory region (up to a distance of 10 wavelengths) was indicated in which contrast thresholds were found to decrease by up to a factor of two. The interactions between the foveal target and the flanking Gabor signals are spatial-frequency and orientation specific in both regions, but less specific in the suppression region. These findings were obtained when the target and masks assumed the same vertical orientation producing collinear configuration, suggesting a possible mechanism for line segmentation, filling-in

gaps, and illusory contours. Indeed, recent studies support the existence of similar interactions involved in integration of line segments (Morgan & Hotopé, 1989; Moulden & Zablocki, 1992; Field, Hayes & Hess, 1993), perception of Glass patterns (Sagi & Kovács, 1993) and in perceiving illusory contours (Dresp & Bonnet, 1991).

The presence of long range lateral connections revealed by intracellular injections of horseradish peroxidase (HRP) (Gilbert & Weisel, 1979, 1983) suggest that visual cortical neurons integrate visual information from a region larger than the classical receptive field. Cross-correlation analysis, indicated excitatory interactions between pairs of cells with similar receptor field orientation preferences (Ts'o & Gilbert, 1988; Ts'o, Gilbert & Weisel, 1986). HRP labeling in the striate cortex of tree shrew, indicated stripe-like zones of neuronal interconnections over considerable distances (Rockland & Lund, 1982). However, between these zones with long interconnections is another set of stripe-like zones which either have shorter or no connections. This led to the suggestion by Mitchison and Crick (1982) that a given cortical cell connects only to other cells of the same or similar orientation preference, and only along an axis in the visual space that is functionally significant for that cell. However, this suggestion is not supported, as of yet, by experimental results revealed from primate visual cortex (see LeVay, 1988).

Here we explore the architecture of spatial interactions using a lateral masking paradigm (Polat & Sagi, 1993). Standard contrast detection tasks were used, under conditions of lateral masking. Three Gabor signals

---

\*Department of Neurobiology, Brain Research, The Weizmann Institute of Science, Rehovot 76100, Israel.

(Gabor, 1946), a Gabor target located in the foveal region between two masking Gabor signals positioned with identical eccentricity, were utilized. Changes in the detection threshold induced by the flanking masking signals as a function of their eccentricity were measured. In our earlier study target and masks were collinear, thus it was not possible to conclude about the architecture of the lateral interactions revealed by this paradigm. Here we vary the global configuration of the three Gabor signals so that the three signals can be parallel, diagonal or orthogonal to the global orientation produced by the triplet (Fig. 1). Previous results for collinear configurations (Polat & Sagi, 1993) show two types of interactions; suppression (threshold elevation of the target in

the presence of the mask), and facilitation (threshold reduction). The documented suppression effect is probably the result of local (within filter) masking and is restricted to distances where the target and masks overlapped, in agreement with earlier studies (Harvey & Doan, 1990; Legge & Foley, 1980; Phillips & Wilson, 1984; Swift & Smith, 1983; Tolhurst & Barfield, 1978; Wilson, McFarlane & Phillips, 1983). However, the observed facilitatory effect reflects a larger range of spatial interactions, probably between filters as implied by the phase insensitivity of the effect (Polat & Sagi, 1993). Herein, enhancement interactions between channels, as a function of their spatial configurations, were examined.

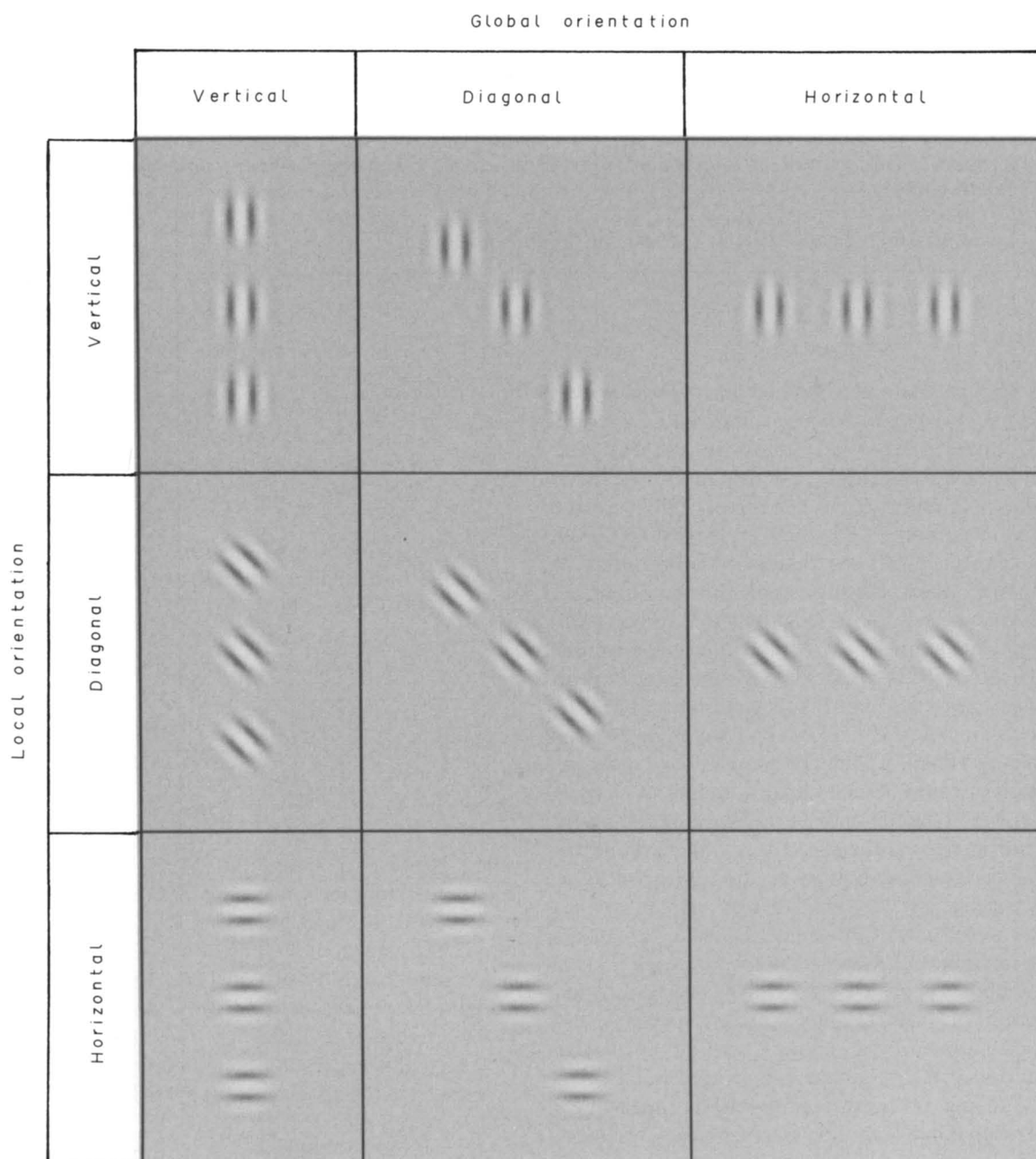


FIGURE 1. The configurations and orientations, both global ( $\theta_g$ ) and local ( $\theta_l$ ) of the stimuli used. (For diagonal  $\theta_g$  we used also  $\theta_l = 135$  deg, however, this configuration is not presented in this figure.) Only one target to mask distance is depicted here, but several were tested. See Methods for more details.

## 2. METHODS

### Apparatus

Stimuli were displayed as graylevel modulation on a Hitachi HM-3619A color monitor, using an Adage 3000 raster display system. The video format was 56 Hz noninterlaced, with  $512 \times 512$  pixels occupying a  $9.6 \times 9.6$  deg area. The mean display luminance [ $I$  in equation (2)] was  $50 \text{ cd/m}^2$  in an otherwise dark environment. Stimulus generation was controlled by a Sun-3/140 workstation and the stimulus display by the Adage local processor. Gamma correction was applied using 10-bit lookup tables.

### Stimuli

Stimuli consisted of three Gabor signals arranged in spatial configurations as depicted in Fig. 1. The luminance distribution [ $L(x, y | x_0, y_0)$ ] of a Gabor signal is determined by

$$L(x, y | x_0, y_0) = \cos\left(\frac{2\pi}{\lambda} ((x - x_0)\cos\theta_1 + (y - y_0)\sin\theta_1)\right) \times \exp\left(-\frac{(x - x_0)^2 + (y - y_0)^2}{\sigma^2}\right) \quad (1)$$

where  $x$  is the value of the horizontal axis,  $y$  of the vertical axis,  $\theta_1$  the orientation of the Gabor signal (in radians),  $\lambda$  the wavelength and  $\sigma$  the standard deviation of the Gaussian envelope. The stimuli used the summation of three Gabor signals shifted by  $\Delta x$  and  $\Delta y$ , [equation (2)] are described by

$$L(x, y | x_0, y_0) = A_m L(x, y | x_0 - \Delta x, y_0 - \Delta y) + A_t L(x, y | x_0, y_0) - A_m L(x, y | x_0 + \Delta x, y_0 + \Delta y) + I. \quad (12)$$

$A_m$  and  $A_t$  are the mask and target amplitudes, respectively. The three Gabor signals were positioned along the vertical, diagonal and horizontal meridians (global orientation,  $\theta_g$ ) by varying  $\Delta x$  and  $\Delta y$ . The orientations of the Gabor signals were controlled by the parameter  $\theta_1$  (local orientation). For each global orientation ( $\theta_g$ ), the local orientations ( $\theta_1$ ) of the three Gabor signals were identical. Only when the local and global orientations coincide ( $\theta_g = \theta_1$ ) is a collinear configuration obtained. In the other configurations used herein the  $\theta_g$  and  $\theta_1$  differed by 45 or 90 deg (Fig. 1). In all the experiments  $x_0, y_0$  coincided with the fixation point. The Gaussian envelope size ( $\sigma = \lambda = 0.075$  deg) was selected so that at least one cycle would be within a range of  $\pm\sigma$  from the Gaussian center. The spatial frequency of the Gabor signal, target and mask, was 13.3 c/deg ( $\lambda = 0.075$  deg). Mask amplitude ( $A_m$ ) was  $0.4 I$  for radial test to mask distances  $> 2\lambda$ , and  $0.32 I$  for smaller distances.

### Experimental procedures

A two-alternative temporal forced-choice paradigm was used. Each block consisted of 48 trials, in which the

signal amplitude and the distance between the Gabor signals were kept constant. Each trial consisted of two stimuli presented sequentially, only one of which had a target. Before each trial, a small fixation cross was presented at the center of the screen. When ready, the observers pushed a key to activate the trial sequence. This sequence consisted of a no stimulus interval ( $360 \pm 270$  msec), a stimulus presentation (90 msec), a no stimulus interval ( $846 \pm 270$  msec), and a second stimulus presentation (90 msec). Screen luminance ( $I$ ) was kept constant during the stimulus and no stimulus intervals. Each stimulus display included two peripheral high contrast crosses ( $3.4 \text{ deg} = 45\lambda$  above and below the fixation cross), marking the target stimulus interval presentation. The observers' task was to determine which of the stimuli contained the target. Auditory feedback, by means of a keyboard bell, was given on observers' error immediately after response. A staircase method was used to determine the contrast threshold. Target contrast was changed every four trials according to the observers' score on the previous four trials: on four correct responses (100% correct) contrast was reduced by 10%, on one error (75% correct) no change was made, on two or more errors (chance level) contrast was increased by 20%. In each block, we set the initial contrast to the contrast threshold as estimated in the previous session. In this procedure, the observers' responses fluctuate around the threshold (75% correct response) during almost all trials in a block. Thresholds were estimated as the average stimulus contrast along a block, ignoring the first eight trials. This procedure was repeated 4–8 times for each stimulus and data presented are averages of these independent estimates (obtained on different days). Some measurements (data not presented here) were made also with fixed stimuli of different contrasts and psychometric curves were generated, yielding practically the same thresholds. In each session either  $\theta_g$  or  $\theta_1$  was kept constant.

### Observers

Three naive observers with normal vision in both eyes, participated in these experiments. The stimuli were viewed binocularly from a distance of 180 cm.

## 3. RESULTS

Data is presented here as the increase in threshold of the flanked target relative to that of an isolated target (log of the ratio of the mask and unmasked contrast thresholds). This presentation allows us to examine effects due to configurations regardless of the local signal orientation which may have different thresholds due to the system anisotropy (absolute thresholds for isolated targets are presented in the figure captions). The distance unit we use is  $\lambda$  (one signal wavelength), since threshold elevation curves as a function of test to mask distance scale with signal wavelength and have the same shape for different wavelengths when distance is measured in  $\lambda$  units (Polat & Sagi, 1993). Typical results, obtained with observer AM using a vertical global orientation ( $\theta_g$ ) are

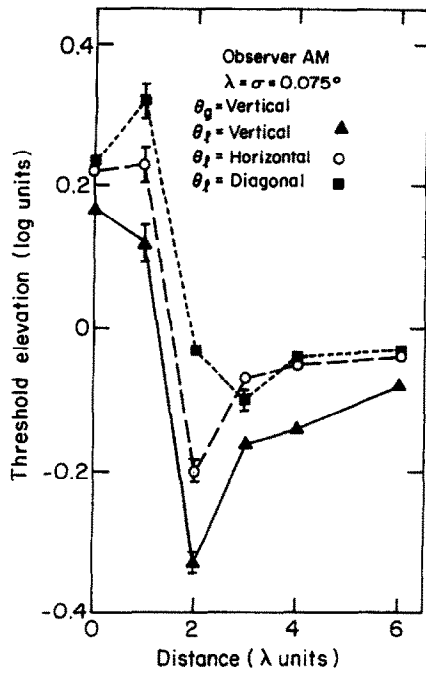


FIGURE 2. Dependence of target threshold on target to mask distance for observer AM ( $\theta_g = \text{vertical}$ ). Threshold elevation was computed relative to that of an isolated target. Isolated target thresholds were  $0.15 I$ ,  $0.16 I$  and  $0.11 I$  for  $\theta_l = \text{vertical}$ , diagonal and horizontal respectively.

depicted in Fig. 2. For vertical local orientation ( $\theta_l$ ) the graph, has the same shape as previously reported (Polat & Sagi, 1993). The threshold reduction (enhancement) magnitude and the range of interactions for each local orientation differ. For instance, maximal effects were obtained with vertical (collinear) orientations, whereas smaller effects were obtained for orthogonal ones and

only a slight enhancement occurred with a diagonal local orientation. Estimates of the maximal enhancement, for  $\theta_g$  (vertical, diagonal and horizontal) as a function of ( $\theta_l$ ) were obtained from graphs like Fig. 2 for three observers (Fig. 3). The main result to note from Fig. 3 (a-c) is that, regardless of global orientation, maximal enhancement was always observed when the global and local orientations coincided ( $\theta_g = \theta_l$ ), i.e. collinear configuration. Less enhancement occurred when  $\theta_g = \theta_l + 90 \text{ deg}$  and when  $\theta_g = \theta_l + 45 \text{ deg}$  the enhancement was only slight.

Another interesting aspect of the data presented in Fig. 3 is that the maximal enhancement magnitude is independent of the isolated target sensitivity. The enhancement values obtained for the different local orientations within the collinear configurations are about the same, although local target thresholds differ. Thus, the parameter affecting enhancement of target detection is the difference between global and local orientations and not some parameter that depends on the observers' orientation sensitivity.

Figure 4 summarizes the results and presents the maximal enhancement obtained from Fig. 3, but now as a function of collinear ( $\theta_g = \theta_l$ ), diagonal ( $\theta_g = \theta_l + 45 \text{ deg}$ ) and orthogonal ( $\theta_g = \theta_l + 90 \text{ deg}$ ) configurations. Collinear configurations are always superior while the diagonal configurations are inferior. The enhancement for collinear configuration is slightly higher when  $\theta_g$  was vertical than horizontal, which probably reflects a spatial interaction asymmetry for collinear configurations. This was most pronounced with observer GH. Practice appeared to increase enhancement when local and global orientations coincided, but not when the orientations differed by 45 deg (Sagi & Polat, 1992). In fact, the asymmetry observed with observer GH disappeared after practice.

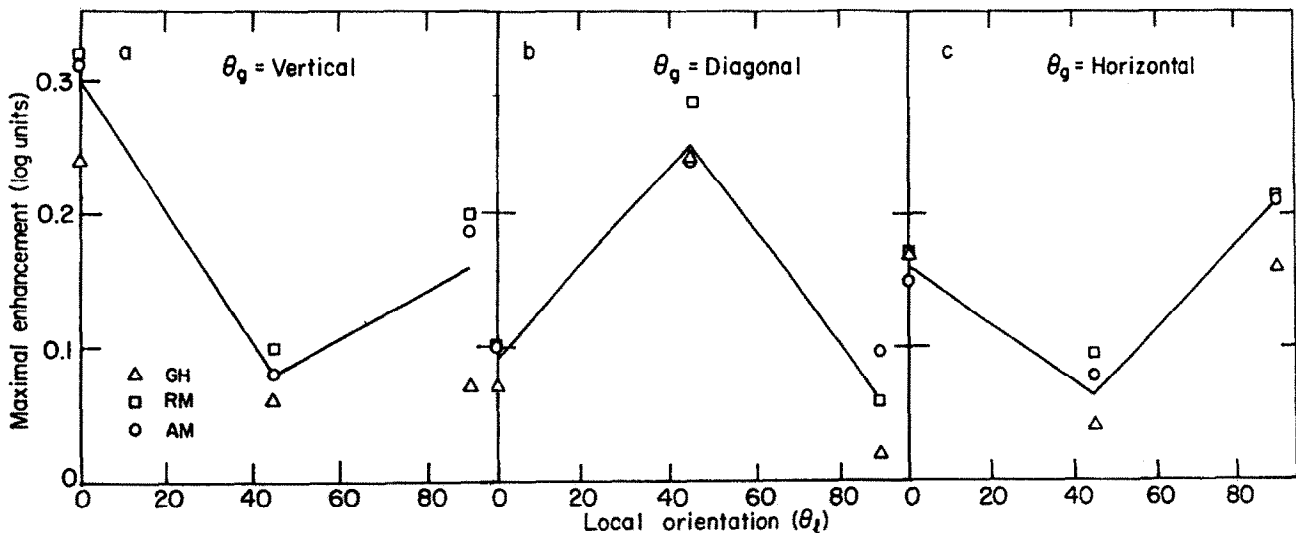


FIGURE 3. Estimates of maximal enhancement for observers AM ( $\circ$ ), RM ( $\square$ ) and GH ( $\triangle$ ) as a function of  $\theta_l$  for vertical (a), diagonal (b) and horizontal (c) ( $\theta_g$ ). The results in (a) were taken from Fig. 2 and in (b, c) from the same type of experiments as described for Fig. 2. The lines depict the average from three observers. The detection threshold amplitude of the isolated target ( $A_t$ ) was for observer AM,  $0.15 I$ ,  $0.16 I$ , and  $0.11 I$  for  $\theta_l = \text{vertical}$ , diagonal, and horizontal respectively; for observer RM,  $0.09 I$ ,  $0.13 I$ , and  $0.13 I$ ; and observer GH,  $0.11 I$ ,  $0.14 I$ , and  $0.10 I$ .

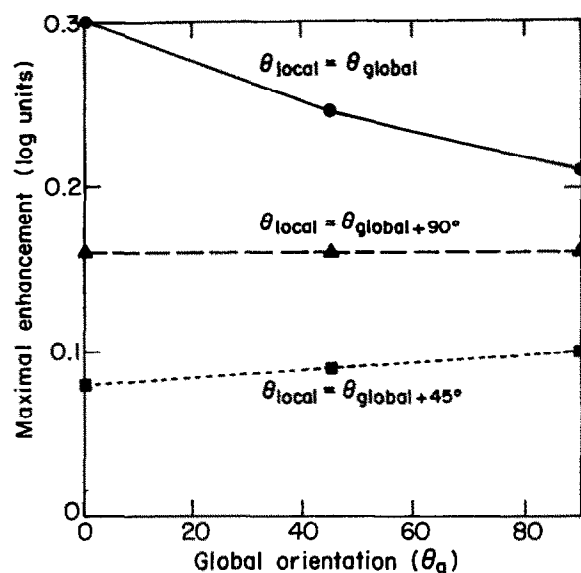


FIGURE 4. Estimates of maximal enhancement for collinear, diagonal, and perpendicular configurations. Data points are the averages of three observers.

#### 4. DISCUSSION

Local spatial interactions involved in visual processes can be explored by monitoring contrast detection of a Gabor target in the presence of high contrast Gabor signals (masks). Sensitivity to the Gabor target can be increased when positioning the two masks at the right distance (Fig. 2; Polat & Sagi, 1993). We report here that the enhancement magnitude and range are a function of the offset between the Gabor target orientation and the direction defined by the virtual line connecting the two masks (Figs 2–4). Effects of a 100 and 50% increase in sensitivity were obtained when this offset was zero and 90 deg, respectively. A 45 deg offset yielded only a small enhancement. This enhancement of sensitivity was independent of the target and masks orientations and locations (meridian).

The pattern of the data obtained (Figs 2–4) suggests that lateral connections are arranged along a main direction that is aligned with the local orientation, less along the orthogonal direction, but not along diagonal directions. Psychophysical measures of illusory contour revealed threshold detection facilitation effect distant from the edges of the inducing elements (Dresp, Free & Bonnet, 1992), but only when the two inducing elements cooperated on the same induction axis. This supports collinear and cooperative boundary completion (Dresp & Bonnet, 1991). Studies of “collector units” (Morgan & Hotopf, 1989; Moulden & Zablocki, 1992), line integration (Field, Hayes & Hess, 1993) and Glass patterns (Sagi & Kovács, 1993) are consistent with the findings presented herein. Recently observers were found to be capable of identifying the path of Gabor signals within randomly oriented elements, when the elements were oriented at angles up to  $\pm 60$  deg relative to one another (Field *et al.*, 1993). Aligning the elements orthogonally reduced the observers’ ability to detect the path. This conforms to the pattern of spatial interactions

observed herein, which suggests a mechanism for line segmentation.

Field *et al.* (1993) claimed that their results for line integration also suggest a mechanism for curvature detection. In further experiments we carried out, when the Gabor target and the flanking masks were aligned along the curved line (Fig. 5) enhancement was not observed (observers AM and UP). Although we used a wide range of curvature parameters, our failure to find evidence for curvature mechanism may be a result of incomplete coverage of the large parameter space. However, note also that the tasks used in the different experiments differ in a significant way. In the experiments described herein, observers had to detect a single Gabor target at threshold, while in those of Field *et al.* (1993) the observers had to follow the path of 12 suprathreshold Gabor signals, thus allowing for a higher level process to take effect.

The architecture of the spatial interactions, as suggested by the results herein and as hypothesized by Mitchison and Crick (1982), may have an important role in tasks involving line segmentations, illusory contours and filling-in gaps. As such, these processes may take part in identifying object contours, however, we do find a significant interaction along the direction orthogonal to this contour. This orthogonal interaction seems to be of the same type as the main axis interaction, although the underlying neural mechanism may differ. Single cell recordings from cat striate cortex indicate the existence of facilitatory interactions along the cell’s main axis and inhibitory interactions in the other directions (Nelson & Frost, 1985). Responses of orientation selective neurons in monkey’s VI area can be suppressed by presenting flanking line segments of similar orientation, on either direction from the cell’s location (Van Essen, DeYoe, Olavarria, Knierim, Fox, Sagi & Julesz, 1989). In this case, our coaxial enhancement may be a result of strong neuronal facilitation, the orthogonal enhancement may

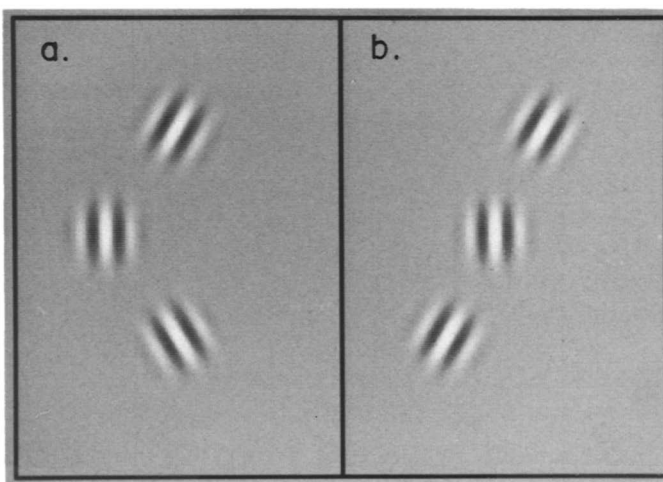


FIGURE 5. Two configurations used to test the sensitivity of a Gabor signal (target) aligned along curvature. Target  $\theta_t$  was vertical and mask  $\theta_m$  was  $\pm 30$  deg (a) or 30 deg (b). Target contrast is enhanced here for illustration. Only one target to mask distance is depicted here, but several were tested.

be a result of disinhibition, and the absence of diagonal interactions may be a result of an inhibitory–excitatory balance.

## REFERENCES

- Cannon, M. & Fullenkamp, S. (1991). Spatial interactions in apparent contrast: Inhibitory effects among grating patterns different spatial frequencies, spatial positions and orientations. *Vision Research*, *31*, 1985–1998.
- Chubb, C., Sperling, G. & Solomon, J. (1989). Texture interactions determine apparent lightness. *Proceedings of the National Academy of Science, U.S.A.* *86*, 9631–9635.
- Dresp, B. & Bonnet, C. (1991). Psychophysical evidence for low-level processing of illusory contours and surfaces in the kanizsa square. *Vision Research*, *31*, 1813–1817.
- Dresp, B., Free, L. & Bonnet, C. (1992). Psychophysical measures of illusory contour information. *Perception (Suppl.)*, *21*, 2.
- Field, D. J., Hayes, A. & Hess, R. F. (1993). Contour integration by the human visual system: Evidence for a local “Association Field”. *Vision Research*, *33*, 173–193.
- Gabor, D. (1946). Theory of communication. *Journal of the Institute of Electrical Engineers, London*, *93*, 429–457.
- Gilbert, C. & Weisel, T. (1979). Morphology and interocortical projections of functionally identified neurons in cat visual cortex. *Nature*, *280*, 120–125.
- Gilbert, C. & Weisel, T. (1983). Clustered intrinsic connections in cat visual cortex. *Journal of Neuroscience*, *3*, 1116–1133.
- Harvey, L. & Doan, V. V. (1990). Visual masking at different polar angles in the two-dimensional fourier plane. *Journal of the Optical Society of America A*, *7*, 116–127.
- Hayes, D. J. F. A. & Hess, R. F. (1993). Good continuation and the association field: Evidence for local feature integration in the visual system. *Vision Research*. Submitted.
- Legge, G. & Foley, J. M. (1980). Contrast masking in human vision. *Journal of the Optical Society of America*, *70*, 1458–1471.
- LeVay, S. (1988). The patchy intrinsic projections of visual cortex. *Progress in Brain Research*, *75*, 147–161.
- Mitchison, G. & Crick, F. (1982). Long axons within the striate cortex: Their distribution, orientation, and pattern of connections. *Proceedings of the National Academy of Science, U.S.A.*, *79*, 3661–3665.
- Morgan, M. J. & Hotopf, W. H. N. (1989). Perceived diagonals in grids and lattices. *Vision Research*, *29*, 1005–1015.
- Moulden, B. & Zablocki, G. (1992). Psychophysical evidence for “collector units”. *Perception (Suppl.)*, *21*, 2.
- Nelson, J. I. & Frost, B. J. (1985). Intracortical facilitation among co-oriented, co-axially aligned simple cells in cat striate cortex. *Experimental Brain Research*, *61*, 54–61.
- Phillips, G. & Wilson, H. (1984). Orientation bandwidths of spatial mechanisms measured by masking. *Journal of the Optical Society of America*, *1*, 226–232.
- Polat, U. & Sagi, D. (1993). Lateral interactions between spatial channels: Suppression and facilitation revealed by lateral masking experiments. *Vision Research*, *33*, 993–999.
- Rockland, K. S. & Lund, J. S. (1982). Widespread periodic intrinsic connections in the tree shrew visual cortex. *Science*, *215*, 1532–1534.
- Sagi, D. (1990). Detection of an orientation singularity in gabor textures: Effect of signal density and spatial-frequency. *Vision Research*, *30*, 1377–1388.
- Sagi, D. & Hochstein, S. (1985). Lateral inhibition between spatially adjacent spatial-frequency channels? *Perception & Psychophysics*, *37*, 315–322.
- Sagi, D. & Kovács, I. (1993). Long range process involved in the perception of glass pattern. *Investigative Ophthalmology Visual Science (Suppl.)*, *34*, 1130.
- Sagi, D. & Polat, U. (1992). Perceptual learning increase the range of inhibitory connections between spatial filters. *Perception (Suppl.)*, *21*, 2.
- Swift, D. S. & Smith, R. A. (1983). Spatial frequency masking and weber’s law. *Vision Research*, *23*, 495–505.
- Tolhurst, D. & Barfield, L. (1978). Interaction between spatial-frequency channels. *Vision Research*, *18*, 951–958.
- Ts’o, D. & Gilbert, C. (1988). The organization of chromatic and spatial interactions in the primate striate cortex. *Journal of Neuroscience*, *8*, 1712–1727.
- Ts’o, D., Gilbert, C. & Weisel, T. (1986). Relationships between horizontal interactions and functional architecture in cat striate cortex as revealed by cross-correlation analysis. *Journal of Neuroscience*, *6*, 1160–1170.
- Van Essen, D. C., DeYoe, E. A., Olavarria, J. F., Knierim, J. J., Fox, J. M., Sagi, D. & Julesz, B. (1989). Neural responses to static and moving texture patterns in visual cortex of the macaque monkey. In Lam, D. M. K. & Gilbert, C. (Eds), *Neural mechanisms of visual perception* (pp. 137–154). Woodlands, Tex.: Portfolio.
- Wilson, H., McFarlane, D. & Phillips, G. (1983). Spatial frequency tuning of orientation selective units estimated by oblique masking. *Vision Research*, *23*, 873–882.